Control of Spin Waves in a Thin Film Ferromagnetic Insulator through Interfacial Spin Scattering

Zihui Wang,[1] Yiyan Sun,[1] Mingzhong Wu,[1,*] Vasil Tiberkevich,[2] and Andrei Slavin[2]
[1]Department of Physics, Colorado State University, Fort Collins, Colorado 80523, USA
[2]Department of Physics, Oakland University, Rochester, Michigan 48309, USA
(Received 12 April 2011; published 29 September 2011)

Control of spin waves in a ferrite thin film via interfacial spin scattering was demonstrated. The experiments used a 4.6 μm-thick yttrium iron garnet (YIG) film strip with a 20-nm thick Pt capping layer. A dc current pulse was applied to the Pt layer and produced a spin current across the Pt thickness. As the spin current scatters off the YIG surface, it can either amplify or attenuate spin-wave pulses that travel in the YIG strip, depending on the current or field configuration. The spin scattering also affects the saturation behavior of high-power spin waves.

DOI: 10.1103/PhysRevLett.107.146602 PACS numbers: 72.25.Ba, 72.25.Mk, 72.25.Rb, 75.30.Ds

Spin waves in ferromagnetic films have many unique properties and thereby have potential for applications in microwave signal processing [1–3], logic operations [4–6], and insulator-based electrical signal transmissions [7]. These applications, however, are bottlenecked by the damping of spin waves. Such damping can result from various physical processes, such as spin-orbit coupling, scattering on defects, and three- and four-wave nonlinear interactions [8].

One way to compensate the spin-wave damping is to use parametric pumping [8], and previous experiments have demonstrated that the spin waves in magnetic thin films could be parametrically amplified [9,10]. This method, however, requires the use of (1) an external microwave signal with a frequency twice that of the spin wave and (2) a delicate microwave resonator for the delivery of this signal to the magnetic film. Moreover, the amplification is limited to a very narrow frequency range, which is determined by the frequency conditions of the parametric resonance.

This Letter reports on a new method for the amplification of spin waves. Specifically, the Letter presents the first demonstration of the electric control of spin waves in a thin film ferromagnetic insulator via interfacial spin scattering (ISS). Experiments use a 4.6 μm-thick yttrium iron garnet (YIG) film strip with a 20-nm thick platinum (Pt) capping layer. A dc current pulse is applied to the Pt film and produces a spin current along the Pt thickness direction via the spin-Hall effect [11–13]. As the spin current scatters off the surface of the YIG film, it exerts a torque on the YIG surface spins. Because of the dipolar and exchange interactions, the effect of this torque is extended to other spins across the YIG thickness and thereby to spin-wave pulses that travel in the YIG film.

The net effect of the ISS process on spin waves depends critically on the relative orientation of (1) the magnetic moments of the electrons in the Pt layer which scatter off the YIG surface and (2) the precession axis of the magnetic moments on the YIG surface. When they are antiparallel, the spin-wave damping is reduced and the amplitude of a traveling spin-wave pulse is increased. In contrast, in a parallel configuration, the spin-wave pulse experiences an enhanced attenuation. The ISS process can also raise or reduce the power level to which high-power spin-wave pulses saturate due to nonlinear damping [8,14]. It is important to emphasize that, as the parallel-antiparallel configuration can be changed simply by reversing the direction of the dc current, this work demonstrates a rather simple new approach for the control of spin waves. One can expect that in the future this ISS effect would allow for the realization of decay-free spin-wave propagation and the development of a new class of electronic devices [1–6].

Figure 1 shows a schematic of the experimental setup. The core component is a long and narrow YIG film strip with its central portion covered by a Pt thin film. The YIG film is magnetized by an in-plane magnetic field H. The field is referred to as a "positive field" ($H > 0$) when it is applied along the $+y$ direction and a "negative field" ($H < 0$) when it is in the $-y$ direction. This film-field configuration supports the propagation of surface spin

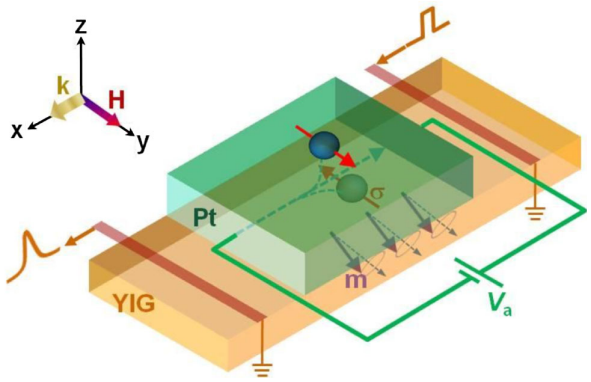

FIG. 1 (color online). Experimental setup for control of spin waves through interfacial spin scattering in a YIG/Pt structure.

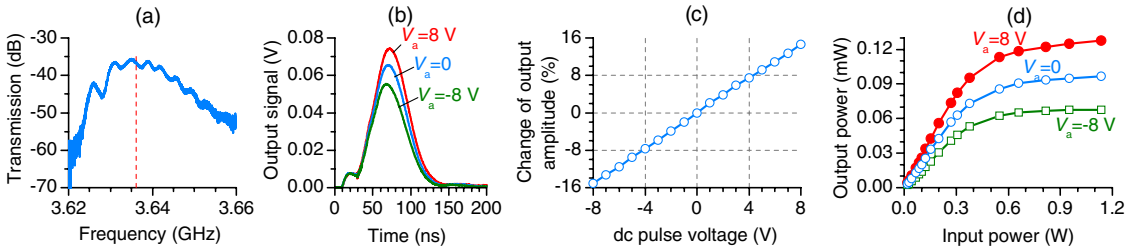

FIG. 2 (color online). Control of spin waves through interfacial spin scattering. (a) Transmission profile for the transducer-YIG-transducer structure. (b) Time-domain output signals for different dc pulse voltages (V_a) applied to the Pt layer. (c) Relative change in output signal amplitude as a function of V_a. (d) Output power versus input power responses for three V_a values, as indicated.

waves, of which the amplitude has an exponential distribution along the YIG film thickness [1,2]. When $H > 0$, the spin wave with a wave vector $\mathbf{k}$ along the $+x$ direction has a larger amplitude near the top surface of the YIG film. When $H < 0$, the spin wave along the $+x$ direction has a larger amplitude near the bottom surface of the YIG film. Two microstrip transducers are placed on the right and left ends of the YIG strip for the excitation and detection, respectively, of the spin wave.

A dc voltage V_a is applied to the Pt film. A positive voltage ($V_a > 0$) results in a current flow along the $+x$ direction and a flow of electrons along the $-x$ direction. The electrical current produces a spin current along the Pt thickness direction via the spin-Hall effect. When $V_a > 0$, the electrons moving towards the YIG film have their magnetic moments in the $-y$ direction. In Fig. 1, the small spheres in the Pt layer represent electrons, and the arrows through the spheres indicate the directions ($\hat{\boldsymbol{\sigma}}$) of the electron magnetic moments.

For the data presented below, the YIG strip was 4.6 μm thick, 2.2 mm wide, and 22 mm long. It was cut from a larger single-crystal (111) YIG film grown on a gadolinium gallium garnet substrate by liquid phase epitaxy. The Pt film was grown on the YIG strip at room temperature by pulsed laser deposition (PLD). Based on the PLD parameters, the thickness of the Pt film was estimated to be about 20 nm. This value matches the estimation based on the resistance of the Pt element, which was 20.1 nm. For this estimation, a resistivity of $\rho = 371$ nΩ m was used for the Pt film [15]. The Pt element had the same width as the YIG strip and a length of $L = 3.5$ mm. The microstrip transducers were 50 μm wide and 2.0 mm long. The transducer separation was held at 5.5 mm, with each transducer 1.0 mm away from the Pt element.

The signals applied to the excitation transducer were microwave pulses with a width of 50 ns and a repetition period of 10 ms. These signals excited spin-wave pulses in the YIG strip. The signals applied to the Pt element were dc pulses with a width of 300 ns and the same period as the microwave pulses. The microwave pulses had a delay of 20 ns relative to the dc pulses. These parameters ensure that the spin current was on over the entire propagation time of each spin-wave pulse.

Figure 2 presents the data measured for $H = 683$ Oe. Figure 2(a) shows the transmission profile for the transducer-YIG-transducer structure. The dashed line indicates a frequency of 3.636 GHz, which was the carrier frequency of the input microwave pulses for most of the measurements. Figure 2(b) shows output signals measured for three different dc pulse voltages (V_a) applied to the Pt layer. The time $t = 0$ corresponds to the moment when a microwave pulse enters the excitation transducer. Figure 2(c) gives the relative change in the peak voltage of the output signal as a function of V_a. Here, the relative change is defined as $(V - V_0)/V_0$, where V_0 is the peak voltage of the output signal for $V_a = 0$ and V is the peak voltage of the output signal for $V_a \neq 0$. For the data in both Figs. 2(b) and 2(c), the power of the input microwave pulses was set to 0.68 W. Figure 2(d) shows the peak power of the output pulse as a function of the peak power of the input microwave pulse for three V_a values.

The data in Fig. 2 show three important results. (1) The application of a positive voltage to the Pt element leads to an enhancement in the amplitude of the output signal and an increase in the power level to which the output pulse saturates. This indicates that, when $V_a > 0$, the ISS effect leads to the amplification of the spin wave and plays a role of negative damping. (2) In contrast, the application of a negative voltage to the Pt element leads to a decrease in both the amplitude and the saturation power level of the output pulse. This indicates that, when $V_a < 0$, the ISS effect results in an attenuation in the spin-wave amplitude and plays a role of additional damping. (3) Over the highest available V_a range, the output signal amplitude versus V_a response shows almost perfect linear behavior. Additionally, the data in Fig. 2(b) also indicate that a "short" pulse travels slightly faster than a "tall" pulse. This can be explained by the nonlinearity-associated dependence of the spin-wave group velocity (v_g) on amplitude [16].

These results can be interpreted as follows. When spin-polarized electrons scatter off the YIG surface, they transfer a certain net angular momentum to the surface spins in the YIG film. This momentum transfer is realized through the s-d exchange interactions at the Pt/YIG interface. Here, s refers to spin-polarized conduction electrons in

the Pt layer, while d refers to localized electrons on the YIG surface. A theoretical model of this interfacial process had been suggested recently [17].

The interfacial momentum transfer results in a net torque on the surface magnetic moments in the YIG film [18,19]:

$$\boldsymbol{\tau} = C\frac{\gamma J_s}{M_s T}\hat{\mathbf{m}} \times \hat{\boldsymbol{\sigma}} \times \hat{\mathbf{m}}, \quad (1)$$

where $\hat{\mathbf{m}}$ is a unit vector along the magnetic moment direction of the YIG surface spins, γ is the absolute value of the gyromagnetic ratio, M_s is the saturation magnetization of the YIG film, T is the effective thickness of the YIG surface layer where the spins are involved in the momentum transfer, and C is a phenomenological coefficient which describes the properties of the Pt/YIG interface such as the spin mixing conductance. J_s is the density of the spin current in the Pt layer and can be written as

$$J_s = \theta_{\mathrm{SH}} J_c = \theta_{\mathrm{SH}} \frac{|V_a|}{\rho L}, \quad (2)$$

where θ_{SH} and J_c are the spin-Hall angle of and the charge current in the Pt element, respectively. The torque $\boldsymbol{\tau}$ is exerted on the surface magnetic moments in the YIG film, but its effect is extended to other moments across the YIG thickness via dipolar and exchange interactions.

One can write the moment vector $\hat{\mathbf{m}}$ as $\mathbf{m}_0 + \mathbf{m}(t)$, where $\mathbf{m}_0$ is along the precession axis and is typically considered to be static and $\mathbf{m}(t)$ is perpendicular to the precession axis and is dynamical. The magnitude of $\mathbf{m}(t)$ defines the spin-wave amplitude. If one takes the small-signal approximation, namely, $|\mathbf{m}(t)| \ll |\mathbf{m}_0|$, one can rewrite Eq. (1) as

$$\boldsymbol{\tau} = \mathrm{sgn}(-\mathbf{m}_0 \cdot \hat{\boldsymbol{\sigma}}) C\frac{\gamma J_s}{M_s T}\mathbf{m}(t). \quad (3)$$

With this equation, one can qualitatively understand the results shown in Fig. 2, as discussed below.

First, when $V_a > 0$, the vector $\hat{\boldsymbol{\sigma}}$ is along the $-y$ direction, as shown in Fig. 1, and the torque $\boldsymbol{\tau}$ is parallel to the moment $\mathbf{m}(t)$ and tends to open up the precession cone. As a result, the spin-wave pulse is amplified and its saturation power level is raised up. Second, when $V_a < 0$, $\hat{\boldsymbol{\sigma}}$ is along the $+y$ direction and $\boldsymbol{\tau}$ is antiparallel to $\mathbf{m}(t)$. The net effect is that the spin-wave pulse is attenuated and saturates to a lower power level. Third, Eqs. (2) and (3) also indicate that $|\boldsymbol{\tau}|$ increases with $|V_a|$. This explains the behavior shown in Fig. 2(c).

The above interpretation was supported by measurements performed with the direction of $\hat{\boldsymbol{\sigma}}$ fixed and the direction of $\mathbf{m}_0$ varied. The representative data are given in Fig. 3. The figure shows $(V - V_0)/V_0$ as a function of V_a. The open circles show the same data as in Fig. 2(c), which were measured for $H = 683$ Oe. The solid circles show the data for $H = -683$ Oe. This "negative field" supports the propagation of spin waves with a wave vector $\mathbf{k}$ near the bottom surface of the YIG film [1,2]. The squares show the data for a field of 1074 Oe in the $+x$ direction. This field orientation supports the propagation of backward volume spin waves [1,2]. For the volume wave measurements, the frequency of the input microwave pulse was 5.036 GHz. All other parameters were the same as cited above.

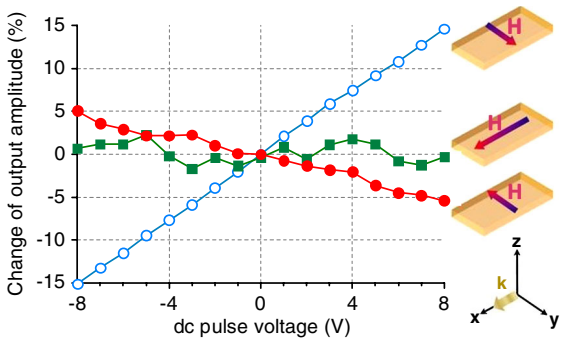

FIG. 3 (color online). Relative change in output pulse amplitude as a function of dc pulse voltage applied to the Pt film for three different field orientations, as indicated.

Three results are evident in Fig. 3. (1) A reversal of the field orientation from the $+y$ direction to the $-y$ direction leads to opposite behavior, and this is true for both $V_a > 0$ and $V_a < 0$. This observation agrees with the expectation of Eq. (3), namely, that a flip of $\mathbf{m}_0$ results in a switching between the $\boldsymbol{\tau} \parallel \mathbf{m}$ and $\boldsymbol{\tau} \parallel (-\mathbf{m})$ configurations and a corresponding switching between the "positive damping" and "negative damping" roles of $\boldsymbol{\tau}$. (2) For a field applied along the length of the YIG strip, the effects of V_a on V are insignificant. This agrees with the prediction of Eq. (1), namely, that the net effect of $\boldsymbol{\tau}$ is zero over each precession period when $\mathbf{m}_0$ and $\hat{\boldsymbol{\sigma}}$ are normal to each other. (3) The ISS effects on the spin waves with larger amplitude near the bottom surface are weaker than those on the waves with larger amplitude near the top surface. This may indicate that the efficiency of transfer of the ISS effects on the surface spins to other spins decreases with film thickness.

Turn now to the evaluation of the ISS-produced changes in the decay rate η and damping constant α of the spin waves. One can use the following equation to model the propagation of a spin-wave pulse $u(x, t)$ along a YIG strip:

$$i\frac{\partial u}{\partial t} = \left[\omega_0 + v_g\left(-i\frac{\partial}{\partial x} - k_0\right)\right]u - i\eta u - i\Delta\eta u, \quad (4)$$

where ω_0 and k_0 are the spin-wave carrier frequency and wave number, respectively. $\Delta\eta$ describes the ISS-produced change in η. It is clear from the above discussion that the sign of $\Delta\eta$ depends on $\mathrm{sgn}(\mathbf{m}_0 \cdot \hat{\boldsymbol{\sigma}})$, and the magnitude of $\Delta\eta$ increases with $|\boldsymbol{\tau}|$ (and thereby with $|V_a|$). To perform the quantitative calculation of $\Delta\eta$, one needs to know the spin mixing conductance at the YIG/Pt interface and consider the specific spin-wave configuration. For the

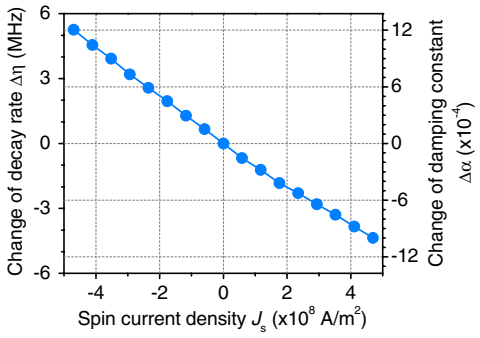

FIG. 4 (color online). Change in spin-wave decay rate and damping constant as a function of spin current density in the Pt layer.

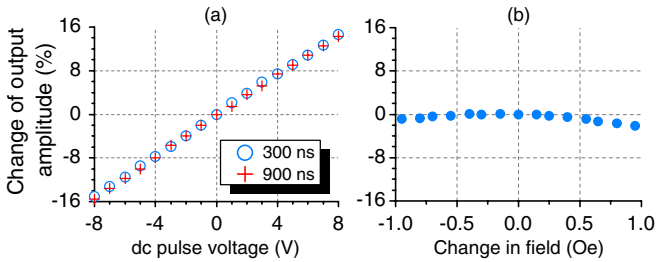

FIG. 5 (color online). (a) Relative change in output pulse amplitude as a function of dc pulse voltage for two dc pulse durations. (b) Relative change in output pulse amplitude as a function of a shift in magnetic field.

qualitative discussion below, one introduces a phenomenological expression

$$\Delta\eta = \mathrm{sgn}(\mathbf{m}_0 \cdot \hat{\boldsymbol{\sigma}})\lambda \frac{\theta_{\mathrm{SH}}|V_a|}{\rho L}, \tag{5}$$

where the coefficient λ describes the efficiency of the change of η due to the ISS process. One can use Eq. (4) to determine the spatial variation of the peak amplitude of the pulse $u(x, t)$. Assuming A_0 and A are the peak amplitudes of $u(x, t)$ at $x = L$ for $V_a = 0$ and $V_a \neq 0$, respectively, one then obtains

$$\frac{A - A_0}{A_0} = e^{-\Delta\eta L/v_g} - 1. \tag{6}$$

This ratio equals $(V - V_0)/V_0$. Thus, one can use the data in Fig. 3 and Eq. (6) to estimate $\Delta\eta$.

Figure 4 gives the ISS-produced changes in η and α for the experimental configurations which are the same as for the data shown in Figs. 2(b) and 2(c). The left and right axes show $\Delta\eta$ and $\Delta\alpha$, respectively, as a function of J_s. The estimation of $\Delta\alpha$ was based on the assumption that η was close to the decay rate of a uniform mode. The estimation used $2\Delta\eta = \Delta\alpha\gamma(2H + 4\pi M_s)$ [20], with $\gamma = 2.8$ MHz/Oe and $4\pi M_s = 1750$ G. The J_s values were obtained with Eq. (2) and $\theta_{\mathrm{SH}} = 0.076$ [19]. The data in Fig. 4 clearly show that one can control, either enhance or mitigate, the decay of a spin wave through the ISS process. Fitting the $\Delta\eta$ values with Eq. (5) yields $\lambda = 1.03 \times 10^{-2}$ m^2 Hz/A for the $H \parallel (+y)$ case and $\lambda = 0.33 \times 10^{-2}$ m^2 Hz/A for the $H \parallel (-y)$ case.

In addition to the spin current, the electric current in the Pt layer also produces Ohmic heating and Oersted fields, but both have negligible influences on spin waves for the configurations in the present work. Figure 5 shows representative data. Figure 5(a) gives $(V - V_0)/V_0$ as a function of V_a. The circles give the same data as in Fig. 2(c), for which the dc pulse width was 300 ns. The crosses give the data measured with a dc pulse width of 900 ns. One sees an almost perfect agreement between the two sets of data. This indicates that the heating effect is very weak. Figure 5(b) gives the relative change of the output amplitude as a function of a small shift in H. The data were measured for $V_a = 0$. Other parameters are the same as cited above. A ± 1 Oe field shift range was considered because the estimated value of the current-produced field was less than 1 Oe. The data in Fig. 5(b) show that the field-induced amplitude change is less than 2%. This small change probably results from the shift of the spin-wave dispersion curve with the field [1,2]. The dispersion shift can give rise to a shift of the transmission profile [see Fig. 2(a)] along the frequency axis and a corresponding change in transmission loss for a specific spin wave.

In conclusion, this Letter reports the first experimental demonstration of the control of spin waves propagating in ferromagnetic insulator films through the ISS process. The experiment utilized a YIG thin film strip with an ultrathin Pt capping layer. It was found that one can control the amplitude and saturation behavior of a spin-wave pulse through the application of a dc pulse to the Pt layer. Future works that are of great interest include the demonstration of much larger amplifications and the development of a rigid theory for the ISS effects. The quasilinear responses shown in Fig. 2(c) are for a relatively small dc pulse voltage range. At higher dc voltage levels, one can expect exponential behavior predicted by Eqs. (5) and (6). In other words, it is possible to realize a much larger amplification of spin waves through the use of higher dc voltages. The increase in amplification will be eventually limited by the heating-caused spin current polarization degradation in the Pt layer and the nonlinear damping of spin waves.

This work was supported in part by the U.S. National Science Foundation (ECCS-0725386, DMR-0906489, ECCS-1001815, and DMR-1015175), the U.S. National Institute of Standards and Technology, and the U.S. Army TARDEC RDECOM. The authors acknowledge Dr. Bretislav Heinrich and Dr. Axel Hoffmann for helpful discussions.

*Corresponding author.
mwu@lamar.colostate.edu

[1] P. Kabos and V. S. Stalmachov, *Magnetostaic Waves and Their Applications* (Chapman and Hall, London, 1994).

[2] D. D. Stancil and A. Prabhakar, *Spin Waves: Theory and Applications* (Springer, New York, 2009).
[3] J. D. Adam *et al.*, IEEE Trans. Microwave Theory Tech. **50**, 721 (2002).
[4] S. Bance *et al.*, J. Appl. Phys. **103**, 07E735 (2008).
[5] T. Schneider *et al.*, Appl. Phys. Lett. **92**, 022505 (2008).
[6] A. Khitun *et al.*, J. Phys. D **43**, 264005 (2010).
[7] Y. Kajiwara *et al.*, Nature (London) **464**, 262 (2010).
[8] A. G. Gurevich and G. A. Melkov, *Magnetization Oscillations and Waves* (CRC Press, New York, 1996).
[9] P. A. Kolodin *et al.*, Phys. Rev. Lett. **80**, 1976 (1998).
[10] A. V. Bagada *et al.*, Phys. Rev. Lett. **79**, 2137 (1997).
[11] M. I. Dyakonov and V. I. Perel, JETP Lett. **13**, 467 (1971).
[12] J. Hirsch, Phys. Rev. Lett. **83**, 1834 (1999).
[13] C. Day, Phys. Today **58** No. 2, 17 (2005).
[14] M. M. Scott *et al.*, J. Appl. Phys. **95**, 6294 (2004).
[15] J. S. Agustsson *et al.*, J. Phys. Conf. Ser. **100**, 082006 (2008).
[16] A. N. Slavin and C. E. Zaspel, J. Appl. Phys. **91**, 8673 (2002).
[17] S. Takahashi, E. Saitoh, and S. Maekawa, J. Phys. Conf. Ser. **200**, 062030 (2010).
[18] K. Ando *et al.*, Phys. Rev. Lett. **101**, 036601 (2008).
[19] L. Liu *et al.*, Phys. Rev. Lett. **106**, 036601 (2011).
[20] D. J. Craik, *Magnetic Oxide* (John Wiley, London, 1975).